

Article

Direct Electrochemistry and Electrocatalysis of Hemoglobin at Mesoporous Carbon Modified Electrode

Supeng Pei ¹, Song Qu ^{2,*} and Yongming Zhang ^{1,*}

¹ School of Chemistry and Chemical Engineering, Shanghai Jiao Tong University, Shanghai 200240, China; E-Mail: peisupeng@sjtu.edu.cn

² College of Science, University of Shanghai for Science and Technology, Shanghai 200093, China

* Authors to whom correspondence should be addressed; E-Mails: qsong@usst.edu.cn (S.Q.); ymzhang@sjtu.edu.cn (Y.M.Z.); Tel.: +86-21-55274547 (S.Q.); +86-21-54742567 (Y.M.Z.); Fax: +86-21-55274547 (S.Q.); +86-21-54742567 (Y.M.Z.).

Received: 30 November 2009; in revised form: 30 December 2009 / Accepted: 18 January 2010 /

Published: 3 February 2010

Abstract: The novel highly ordered mesoporous carbon (known as FDU-15), prepared by the organic-organic self-assembly method was been used for first time for the immobilization of hemoglobin (Hb) and its bioelectrochemical properties were studied. The resulting Hb/FDU-15 film provided a favorable microenvironment for Hb to perform direct electron transfers at the electrode. The immobilized Hb also displayed its good electrocatalytic activity for the reduction of hydrogen peroxide. The results demonstrate that mesoporous carbon FDU-15 can improve the Hb loading with retention of its bioactivity and greatly promote the direct electron transfer, which can be attributed to its high specific surface area, uniform ordered porous structure, suitable pore size and biocompatibility. Our present study may provide an alternative way for the construction of nanostructure biofunctional surfaces and pave the way for its application to biosensors.

Keywords: hemoglobin; mesoporous carbon; direct electron transfer

1. Introduction

The realization of direct electron transfer between the native redox protein and the underlying electrode is significantly important because it not only provides models for studying the mechanism of

biological electron transport, but also enables construction of mediator-free biosensors and bioreactors [1,2]. Hemoglobin (Hb) is a heme protein which can store and transport oxygen in the blood in vertebrates. Because of its commercial availability and well-documented structure, Hb is an ideal model molecule for the study of direct electron transfer reactions and electrocatalysis of heme proteins. However, because of its large structure, it is difficult for Hb to directly exchange electrons with an electrode surface. Therefore, developing suitable materials and methods for effective Hb immobilization on electrode surface is important for achieving their direct electrochemical reactions and retaining their bioactivities. During the past two decades, great efforts have been made to increase the electron transfer kinetics of Hb [3-10].

Mesoporous materials offer new possibilities for immobilization of proteins because they are porous materials with extremely high surface areas and uniform pores [6,11-13]. Mesoporous carbon materials with ordered pore structure, high pore volume, high specific surface area, and tunable pore diameters have been widely investigated in various areas such as catalyst supports, electrode materials, molecular separation and so on [14-17]. In particular, the ordered mesoporous carbon materials also have been widely applied in electrochemical biosensors [18-20].

The ordered mesoporous carbon materials have been usually prepared by the nanocasting method using hard-templates [21]. Recently, a direct synthesis of ordered mesoporous carbons through an organic-organic self-assembly method was applied to prepare some ordered mesoporous carbon materials [22-24]. The pore wall structures of these carbons are different from those of mesoporous carbon prepared from nanocasting method using hard templates. For example, a two dimensional (2-D) hexagonal mesostructured carbon FDU-15 prepared by Zhao *et al.* possess continuous and open frameworks with ultrahigh thermal stability in inert atmospheres, which arises from the covalently bonded construction, amorphous carbon components and thick pore walls [22]. These carbonaceous materials possess high surface area, large pore volumes and uniform pore structure. Considering their especial properties, the ordered mesostructured FDU-15 carbons could be used as attractive materials for protein immobilization.

In this report, the highly ordered mesoporous carbon FDU-15 was used for Hb immobilization and then its bioelectrochemical properties were studied. The direct electron transfer of Hb was observed on the Hb/FDU-15 modified electrode. The resulting film provided a desirable microenvironment to retain the bioactivity of Hb. The electrocatalytic reduction of H₂O₂ at the modified electrode was also investigated. It represents a general method for the construction of biosensor and can be applied to other biosystems.

2. Experimental

2.1. Reagents

Pluronic F127 triblock poly(ethyleneoxide)-b-poly(propylene oxide)-b-poly(ethylene oxide) copolymer (MW = 12,600, EO106PO70EO106) was purchased from Acros Corp. Hb (MW 66,000, from bovine blood) was purchased from Shanghai Biochemical Reagent and used without further purification. Other chemicals were purchased from Shanghai Chemical Company. All these chemicals

were used of analytical grade or higher and used as received. All the solutions were prepared with doubly distilled water.

2.2. Syntheses of mesoporous carbon FDU-15

Mesoporous carbon FDU-15 with 2-D hexagonal structures was synthesized through an organic–organic self-assembly method, according to the literature [22]. Briefly, 1.0 g of F127 block copolymer was dissolved in 20.0 g of ethanol. Then 5.0 g of the resol precursors in ethanol solution containing 0.60 g of phenol and 0.45 g of formaldehyde were added under stirring. The homogeneous solution was poured into several dishes to evaporate ethanol at room temperature for 8 h and then heated at 100 °C for 24 h. The as-prepared products were calcined in a tubular furnace under a high purity N₂ atmosphere at 900 °C for 3 h.

2.3. Electrode modification

One mg of mesoporous carbon FDU-15 was dispersed in 1 mL dimethylformamide (DMF) with the aid of ultrasonic agitation to give a 1 mg mL⁻¹ black suspension. 5 mg mL⁻¹ Hb solution was prepared by dissolving Hb in 0.10 M phosphate buffer solution (PBS) at pH 7.0. Prior to modification, the bare glassy carbon (GC) electrode was polished with 0.05 μm alumina slurry and then ultrasonically cleaned in ethanol and water, followed by thoroughly rinsing with water. Then 10 μL of the suspension was spread on the pretreated GCE surface and allowed to dry under an infrared lamp. The mesoporous carbon FDU-15 electrode obtained was thoroughly rinsed with water and immersed in a 5 mg mL⁻¹ Hb solution for 24 h to give the Hb/FDU-15 modified electrode.

2.4. Apparatus and measurements

Transmission electron microscopy (TEM) micrographs of samples were taken using a JEM-2011 electron microscope (JEOL, Japan), with an accelerating voltage of 200 kV. Small-angle X-ray scattering (SAXS) measurements were taken on a Nanostar U smallangle X-ray scattering system (Bruker, Germany) using Cu Ka radiation (40 mV, 35 mA). N₂ adsorption was measured using a Micromeritics Tristar 3000 automatic physisorption instrument at 77 K. The specific surface area was determined by the BET method. The BJH model was used to determine the pore size distribution. The UV-Vis spectras were measured with a JASCO UV550 UV–Vis absorption spectrometer.

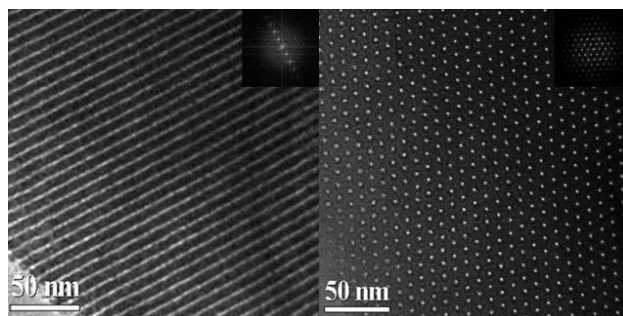
Electrochemical experiments were performed on a CHI 660 electrochemical workstation (CHI, USA) with conventional three-electrode system. The working electrode was a modified GC electrode. A saturated calomel electrode (SCE) and a platinum electrode were used as the reference and the auxiliary electrode, respectively. A 0.10 M PBS was used as the supporting electrolyte. All experimental solutions were deoxygenated by purging pure N₂ into the solution for about 15 min, and N₂ gas was kept flowing over the solution during the electrochemical measurements.

3. Results and Discussion

3.1. Characterization of FDU-15

Transmission electron microscopy (TEM) images of mesoporous carbon FDU-15 (Figure 1) show well ordered stripe-like and hexagonally arranged patterns that are similar to mesoporous silica SBA-15, further confirming a 2D ordered hexagonal mesostructure [25]. The wall thickness is estimated to be 4.0 nm.

Figure 1. TEM images of the mesoporous carbon FDU-15.



SAXS patterns (Figure 2) show that the two-dimensional (2D) hexagonal structure (p6 mm) with three distinct reflection peaks indexed to 10, 11 and 20 respectively. The N₂ sorption isotherms (shown as circles in Figure 3) of the mesoporous carbon FDU-15 yield a type-IV curve with a sharp capillary condensation step at $P/P_0 = 0.4 - 0.6$ and an H₁-type hysteresis loop which is typical of large-pore mesoporous materials with cylindrical channels, according to the International Union of Pure and Applied Chemistry (IUPAC) nomenclature [26]. These results suggest that mesoporous carbon FDU-15 has uniform cylindrical mesoporous channels. The BET surface area and the total pore volume are calculated to be 960 m² g⁻¹ and 0.55 cm³ g⁻¹, respectively. The pore diameter is about 3.4 nm with a narrow distribution.

Figure 2. SAXS patterns of the mesoporous carbon FDU-15.

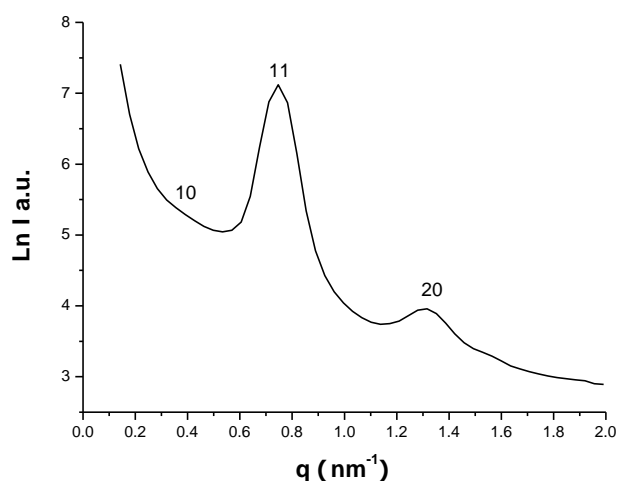
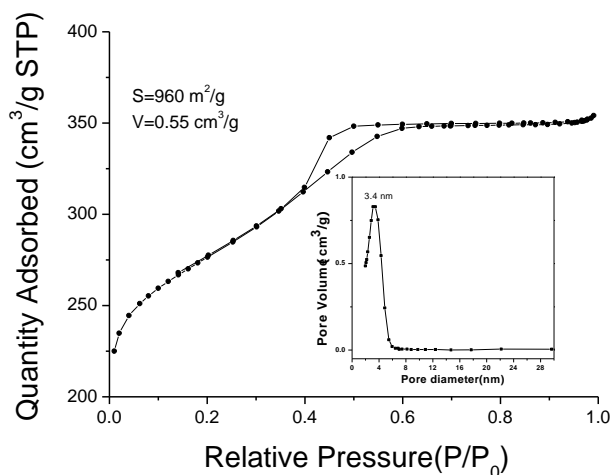


Figure 3. N₂ adsorption curves of the mesoporous carbon FDU-15.

3.2. Direct electrochemistry of Hb on Hb/FDU-15 electrode

Cyclic voltammetry was employed to investigate the Hb/FDU-15 film over the potential range from 0 to -0.6 V. Figure 4 shows the cyclic voltammograms of mesoporous carbon FDU-15/GC and Hb/FDU-15 electrodes at a scan rate of 100 mV s^{-1} , respectively. As compared to GC electrode (not shown), the electrochemical response current at the FDU-15/GC modified electrode is much larger. It can be attributed to the electrode surface area of FDU-15/GC modified electrode is significant increment. The similar phenomenon could be also observed at CNTs modified electrode [27].

No peak was observed at mesoporous carbon FDU-15 (curve a) modified electrode, which showed mesoporous carbon FDU-15 was electroinactive within the potential window. However, a pair of well-defined, nearly symmetrical redox peaks is observed at the Hb/FDU-15 electrode (curve b). The anodic peak potential (E_{pa}) and cathodic peak potential (E_{pc}) are located at -0.304 and -0.357 V, respectively. The formal potential (E^0), estimated as the average of E_{pa} and E_{pc} , is -0.33 V. The peak-to-peak separation (ΔE_p) of 53 mV is observed, which indicates a fast direct electron transfer of Hb in the film. This is in accordance with the characteristic of Fe(III)/Fe(II) redox couples of heme proteins.

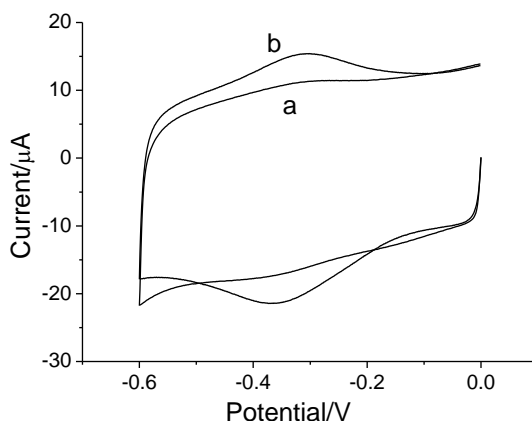
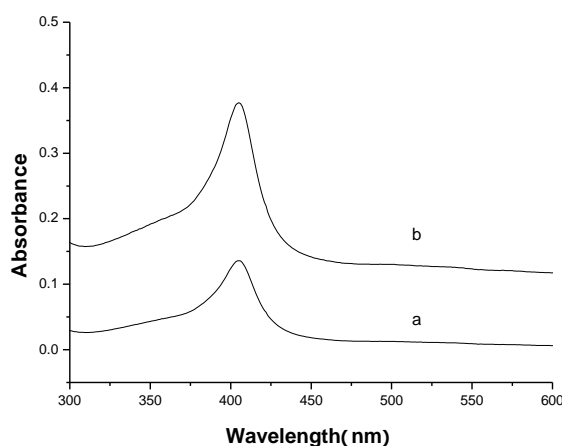
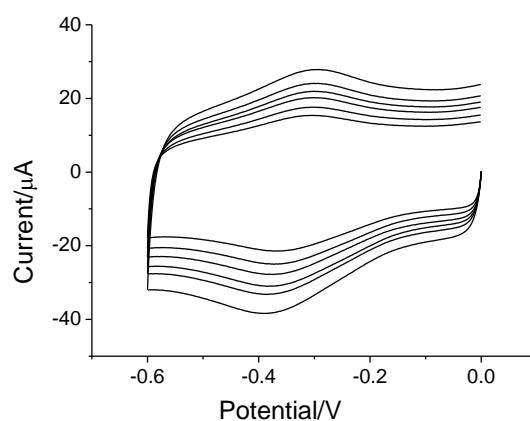
Figure 4. Cyclic voltammograms of (a) FDU-15 and (b) Hb/FDU-15 electrodes in pH 7.0 PBS; scan rate: 100 mV s^{-1} .

Figure 5. UV-Vis spectroscopy of (a)Hb/FDU-15 film and (b)Hb in pH 7.0 PBS.

The direct electrochemistry of Hb indicates that the ordered mesoporous carbon FDU-15 film has good affinity for proteins. Hb has been adsorbed or entrapped by the film for the film porosity. Moreover, the film could greatly facilitate the electrode reaction kinetics of Hb, and provide a favorable microenvironment for electron transfer between Hb and electrode.

Figure 5 shows the UV-Vis spectrum of the Hb/FDU-15 film. It can be observed that the Soret band of the native Hb is located at 403 nm (Figure 5b). After Hb is immobilized, the Soret band is still appeared at 403 nm and the wavelength has no obvious shifted (Figure 5a). The absorption peak at 403 nm is the characteristic Soret-band absorbance of the heme of Hb [28], indicating that the FDU-15 can provide a microenvironment for Hb to retain its native structure.

The influence of scan rate on the response of immobilized Hb in the film was investigated (Figure 6). The linear regression equations of peak current with scan rate is: $I_{pa}(\mu\text{A}) = 0.038 + 0.033 v$ (mV s^{-1}) $I_{pc}(\mu\text{A}) = 0.012 + 0.037 v$ (mV s^{-1}).

Figure 6. Cyclic voltammograms of Hb/FDU-15 modified electrode in pH 7.0 PBS at scan rate of 100, 125, 150, 175, 200 and 250 mV s^{-1} .

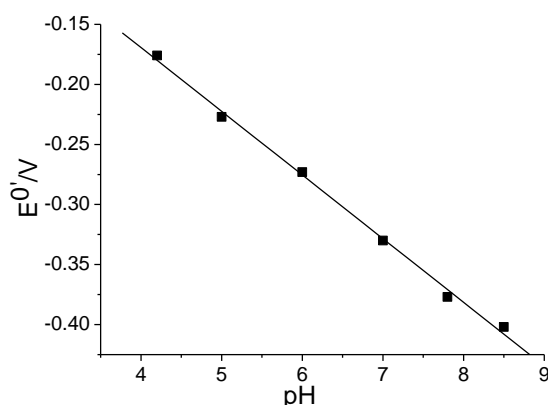
Both the anodic and cathodic peak currents increase linearly with the scan rates (from 100 mV s^{-1} to 250 mV s^{-1}), indicating that the reaction is a surface controlled electrochemical process. According to the slope of the I_p - v curve of $I_p = n^2 F^2 v \Gamma / 4RT$ [29], the average surface coverage (Γ) of Hb was estimated to be $7.17 \times 10^{-11} \text{ mol cm}^{-2}$, which is higher than that of the theoretical monolayer

coverage ($1.89 \times 10^{-11} \text{ mol cm}^{-2}$) [30]. The high loading of Hb is attributed to the porous structure of the ordered mesoporous carbon FDU-15 with its large specific surface area.

When the scan rates increase, the E_{pa} and E_{pc} shift slightly to the positive and the negative directions, respectively. The electrode reaction becomes irreversible at higher scan rates. Using Laviron's equation [31,32], the heterogeneous electron transfer rate constant k of Hb can be calculated as 1.8 s^{-1} .

The effect of pH on the peak potential of Hb immobilized in the film was investigated in different buffer solutions. The dependence of $E^{0'}$ on the pH at the Hb/FDU-15 electrode is shown in Figure 7. It can be observed that the peak potential is obviously dependent on the pH value in the range of 4.0–9.0. The $E^{0'}$ of Hb shifts linearly to the negative direction with increasing pH value with a slope of -53 mV pH^{-1} . The slope of the $E^{0'}$ -pH plots are consistent with the mechanism in which a proton and an electron are transferred per heme group in the electrode reaction.

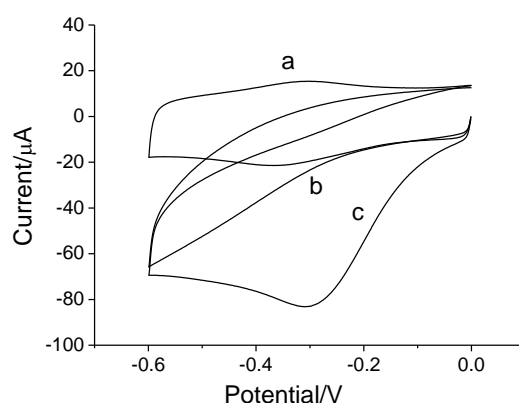
Figure 7. The dependence of $E^{0'}$ of the Hb/FDU-15 electrode on the solution pH.



3.3. Electrocatalysis of H_2O_2 on Hb/FDU-15 electrode

Hb has the ability to catalyze the reduction of H_2O_2 . Figure 8 shows the cyclic voltammograms of the FDU-15 (curve b) and Hb/FDU-15 (curve c) electrode in 0.1 M PBS (pH 7.0) in the presence of H_2O_2 .

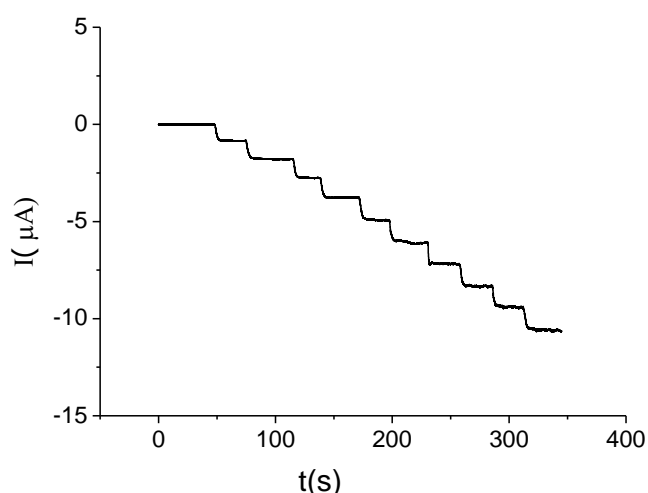
Figure 8. Cyclic voltammograms of the Hb/FDU-15 electrode in 0.1 M PBS (pH 7.0) (curve a); the FDU-15 electrode (b) and the Hb/FDU-15 electrode (c) in the presence of 0.5 mM H_2O_2 . Scan rate: 100 mV s^{-1} .



As for Hb/FDU-15 electrode, in the absence of H_2O_2 , a pair of the redox peaks of Hb is observed (curve a). However, in the presence of H_2O_2 , the voltammetric behavior changes drastically. A large cathodic current for the reduction of H_2O_2 appears while the anodic peak decreases till disappears completely. Compared with that, at FDU-15 electrode, no voltammetry response is observed in the same condition. The results indicate that H_2O_2 exhibits excellent reactivity in the electrocatalysis on the Hb/FDU-15 electrode. The porous structure of mesoporous carbon FDU-15 can provide sufficient space to immobilize Hb and give the immobilized Hb a suitable micro-environment to keep their biological activity.

An attractive feature of the Hb/FDU-15 electrode is the highly stable amperometric response to H_2O_2 . Figure 9 shows the typical steady-state current responses of the modified electrode by the successive addition of $10 \mu M H_2O_2$ at $-0.3 V$.

Figure 9. Typical steady-state current responses of the Hb/FDU-15 electrode on successive addition of $10 \mu M H_2O_2$. Applied potential: $-0.3 V$.



The current responses to the addition of H_2O_2 quickly and sensitively and reaches a steady state in 4 s. Such a fast response can be attributed to the fast diffusion process and a high activity of the Hb in this system. The current is linear with the H_2O_2 concentration from $2 \times 10^{-6} M$ to $3 \times 10^{-4} M$ with the detection limit of $8 \times 10^{-7} M$ ($S/N = 3$). Compared with other CNTs-based H_2O_2 biosensors [33,34], the linear range of our proposed biosensor is broader by about one order of magnitude of H_2O_2 concentration with a markedly lower detection limit. That indicates the hydrogen peroxide biosensor based on Hb/FDU-15 would exhibit more advantageous analytical performance. This improved analytical performance is because FDU-15 has the ability to promote the electron transfer between proteins and electrode.

When the concentration of H_2O_2 is higher than $5 \times 10^{-4} M$, a response plateau is observed, showing the characteristics of the Michaelis–Menten kinetic mechanism. The apparent Michaelis–Menten constant (K_m), which is an indication of the enzyme–substrate kinetics, can be calculated using the Lineweaver–Burk equation(1) [35]:

$$\frac{1}{i} = \frac{1}{I_{\max}} + \frac{K_m^{app}}{I_{\max}} \cdot \frac{1}{C_{H_2O_2}} \quad (1)$$

Accordingly, the K_m value for the Hb/FDU-15 modified electrode is estimated to be 1.38 mM. This value is smaller than that of Hb/CNTs modified electrode [36]. The low value of K_m indicates that Hb immobilized in FDU-15 films retains its bioactivity and has a high biological affinity to H_2O_2 with a low diffusion barrier.

The repeatability and stability of the proposed electrode were studied. The relative standard deviation (RSD) is 3.6% for ten successive measurements of 10 μM H_2O_2 , showing the proposed electrode possesses a good reproducibility. On the other hand, the storage stability of the proposed electrode was also studied. The response current of the electrode decreased to 90% after stored 30 days at 4 °C in a refrigerator. The good long-term stability demonstrated that the FDU-15 film was suitable matrix for immobilization of Hb to retain its activity and prevent it from leaking out of the film.

4. Conclusions

An application of mesoporous carbon FDU-15 in bioelectrochemical research has been studied. Mesoporous carbon FDU-15 possesses high specific surface, ordered pore structure, high pore volume. Thus mesoporous carbon FDU-15 could be used as an attractive materials for protein immobilization. Hb immobilized in the Hb/FDU-15 film has performed direct electrochemistry and retained high electrocatalytic efficiency toward H_2O_2 . The Hb/FDU-15 electrode exhibited good analytical performance features, such as a wide determination range and low detection limit for H_2O_2 determination. Thus, mesoporous carbon FDU-15 as support for redox protein immobilization has potential applications in the fabrication of third-generation biosensors.

Acknowledgements

This work was financially supported by the National High Technology Research and Development Program (“863” Program, No. 2006AA03Z216) and the “11th 5-year” National Key Technologies R&D Program (No. 2006BAE02A00). This work was also supported by Shanghai Municipal Education Commission (No. slg08019).

References

1. Kong, J.; Lu, Z.; Lvov, Y.M.; Desamero, R.Z.A.; Frank, H.A.; Rusling, J.F. Direct electrochemistry of cofactor redox sites in a bacterial photosynthetic reaction center protein. *J. Am. Chem. Soc.* **1998**, *120*, 7371–7372.
2. Willner, I.; Katz, E. Integration of layered redox proteins and conductive supports for bioelectronic applications. *Angew. Chem. Int. Ed.* **2000**, *39*, 1180–1218.
3. Sun, H.; Hu, N.; Ma, H. Direct electrochemistry of hemoglobin in polyacrylamide hydrogel films on pyrolytic graphite electrodes. *Electroanalysis* **2000**, *12*, 1064–1070.
4. Li, Q.; Luo, G.; Feng, J. Direct electron transfer for heme proteins assembled on nanocrystalline TiO_2 film. *Electroanalysis* **2001**, *13*, 359–363.

5. Han, X.; Huang, W.; Jia, J.; Dong, S.; Wang, E. Direct electrochemistry of hemoglobin in egg-phosphatidylcholine films and its catalysis to H₂O₂. *Biosens. Bioelectron.* **2002**, *17*, 741–746.
6. Dai, Z.; Liu, S.Q.; Ju, H.X.; Chen, H.Y. Direct electron transfer and enzymatic activity of hemoglobin in a hexagonal mesoporous silica matrix. *Biosens. Bioelectron.* **2004**, *19*, 861–867.
7. Liu, J.Q.; Chou, A.; Rahmat, W.; Paddon-Row, M.N.; Gooding, J.J. Achieving direct electrical connection to glucose oxidase using aligned single walled carbon nanotube arrays. *Electroanalysis* **2005**, *17*, 38–46.
8. Zhao, Y.D.; Bi, Y.H.; Zhang, W.D.; Luo, Q.M. The interface behavior of hemoglobin at carbon nanotube and the detection for H₂O₂. *Talanta* **2005**, *65*, 489–494.
9. Krajewska, A.; Radecki, J.; Radecka, H. A voltammetric biosensor based on glassy carbon electrodes modified with single-walled carbon nanotubes/hemoglobin for detection of acrylamide in water extracts from potato crisps. *Sensors* **2008**, *8*, 5832–5844.
10. Li, H.H.; Liu, S.Q.; Dai, Z.H.; Bao, J.C.; Yang, X.D. Applications of nanomaterials in electrochemical enzyme biosensors. *Sensors* **2009**, *9*, 8547–8561.
11. Zhang, L.; Zhang, Q.; Li, J.H. Direct electrochemistry and electrocatalysis of hemoglobin immobilized in bimodal mesoporous silica and chitosan inorganic-organic hybrid film. *Electrochem. Commun.* **2007**, *9*, 1530–1535.
12. Chen, C.C.; Do, J.S.; Gu, Y.S. Immobilization of HRP in mesoporous silica and its application for the construction of polyaniline modified hydrogen peroxide biosensor. *Sensors* **2009**, *9*, 4635–4648.
13. Lei, C.H.; Valenta, M.M.; Sparipalli, K.P.; Ackerman, E.J. Biosensing paraoxon in simulated environmental samples by immobilized organophosphorus hydrolase in functionalized mesoporous silica. *J. Environ. Qual.* **2007**, *36*, 233–238.
14. Subramoney, S. Novel nanocarbons-structure, properties, and potential applications. *Adv. Mater.* **1998**, *10*, 1157–1171.
15. Shiflett, M.B.; Foley, H.C. Ultrasonic Deposition of high-selectivity nanoporous carbon membranes. *Science* **1999**, *285*, 1902–1905.
16. Flandrois, S.; Simon, B. Carbon materials for lithium ion rechargeable batteries. *Carbon* **1999**, *37*, 165–180.
17. Chai, G.S.; Shin, I.S.; Yu, J.S. Synthesis of ordered, uniform, macroporous carbons with mesoporous walls templated by aggregates of polystyrene spheres and silica particles for use as catalyst supports in direct methanol fuel cells. *Adv. Mater.* **2004**, *16*, 2057–2061.
18. Zhou, M.; Shang, L.; Li, B.L.; Huang, L.J.; Dong, S.J. Highly ordered mesoporous carbons as electrode material for the construction of electrochemical dehydrogenase- and oxidase-based biosensors. *Biosens. Bioelectron.* **2008**, *24*, 442–447.
19. Zhu, L.D.; Tian, C.Y.; Zhu, D.X.; Yang, R.L. Ordered mesoporous carbon paste electrodes for electrochemical sensing and biosensing. *Electroanalysis* **2008**, *20*, 1128–1134.
20. Lu, X.B.; Xiao, Y.; Lei, Z.B.; Chen, J.P.; Zhang, H.J.; Ni, Y.W.; Zhang, Q. A promising electrochemical biosensing platform based on graphitized ordered mesoporous carbon. *J. Mater. Chem.* **2009**, *19*, 4707–4714.

21. Ryoo, R.; Joo, S.H.; Jun, S. Synthesis of highly ordered carbonmolecular sieves *via* template-mediated structuraltransformation. *J. Phys. Chem. B* **1999**, *103*, 7743–7746.
22. Meng, Y.; Gu, D.; Zhang, F.Q.; Shi, Y.F.; Yang, H.F.; Li, Z.; Yu, C.Z.; Tu, B.; Zhao, D.Y. Ordered mesoporous polymers and homologous carbon frameworks: amphiphilic surfactant templating and direct transformation. *Angew. Chem. Int. Edit.* **2005**, *44*, 7053–7059.
23. Zhang, F.Q.; Meng, Y.; Gu, D.; Yan, Y.; Yu, C.Z.; Tu, B.; Zhao, D.Y. A facile aqueous route to synthesise highly ordered mesoporous polymer and carbon frameworks with Ia-3d bicontinuous cubic structure. *J. Am. Chem. Soc.* **2005**, *127*, 13508–13509.
24. Tanaka, S.; Nishiyama, N.; Egashira, Y.; Ueyama, K. Synthesis of ordered mesoporous carbons with channel structure from an organic-organic nanocomposite. *Chem. Commun.* **2005**, *16*, 2125–2127.
25. Zhao, D.Y.; Feng, J.L.; Huo, Q.S.; Melosh, N.; Fredirckson, G.H.; Chemlka, B.F.; Stucky, G.D. Triblock Copolymer Syntheses of mesoporous silica with periodic 50 to 300 angstrom pores. *Science* **1998**, *279*, 548–552.
26. Sing, K.S.W.; Everett, D.H.; Haul, R.A.W.; Moscow, L.; Pierotti, R.A.; Rouquerol, T.; Siemienewska, T. Reporting physisorption data for gas/solid systems with special reference to the determination of surface area and porosity. *Pure Appl. Chem.* **1985**, *57*, 603–619.
27. Wang, J.X.; Li, M.X.; Shi, Z.J.; Li, N.Q.; Gu, Z.N. Direct electrochemistry of cytochrome *c* at a glassy carbon electrode modified with single-wall carbon nanotubes. *Anal. Chem.* **2002**, *74*, 1993–1997.
28. Liu, S.; Chen, A. Coadsorption of horseradish peroxidase with thionine on TiO₂ nanotubes for biosensing. *Langmuir* **2005**, *21*, 8409–8413.
29. Zhao, G.; Feng, J.; Xu, J.; Chen, H.Y. Direct electrochemistry and electrocatalysis of heme proteins immobilized on self-assembled ZrO₂ film. *Electrochem. Commun.* **2005**, *7*, 724–729.
30. Xian, Y.Z.; Xian, Y.; Zhou, L.H.; Wu, F.H.; Ling, Y.; Jin, L.T. Encapsulation hemoglobin in ordered mesoporous silicas: Influence factors for immobilization and bioelectrochemistry. *Electrochem. Commun.* **2007**, *9*, 142–148.
31. Laviron, E. The use of linear potential sweep voltammetry and of a.c. voltammetry for the study of the surface electrochemical reaction of strongly adsorbed systems and of redox modified electrodes. *J. Electroanal. Chem.* **1979**, *100*, 263–270.
32. Laviron, E. General expression of the linear potential sweep voltammogram for a surface redox reaction with interactions between the adsorbed molecules: Applications to modified electrodes. *J. Electroanal. Chem.* **1980**, *115*, 65–74.
33. Zhao, Y.D.; Bi, Y.H.; Zhang, W.D.; Luo, Q.M. The interface behavior of hemoglobin at carbon nanotube and the detection for H₂O₂. *Talanta* **2005**, *65*, 489–494.
34. Zhao, G.C.; Yin, Z.Z.; Zhang, L.; Wei, X.W. Direct electrochemistry of cytochrome *c* on a multi-walled carbon nanotubes modified electrode and its electrocatalytic activity for the reduction of H₂O₂. *Electrochem. Commun.* **2005**, *7*, 256–260.
35. Kamin, R.A.; Wilson, G.S. Rotating ring-disk enzyme electrode for biocatalysis kinetic studies and characterization of the immobilized enzyme layer. *Anal. Chem.* **1980**, *52*, 1198–1205.

36. Cai, X.; Chen, J. Direct electron transfer and bioelectrocatalysis of hemoglobin at a carbon nanotube electrode. *Anal. Biochem.* **2004**, *325*, 285–292.

© 2010 by the authors; licensee Molecular Diversity Preservation International, Basel, Switzerland. This article is an open-access article distributed under the terms and conditions of the Creative Commons Attribution license (<http://creativecommons.org/licenses/by/3.0/>).